



**HAL**  
open science

## Small-Molecule Inhibitors of Cyclophilins Block Opening of the Mitochondrial Permeability Transition Pore and Protect Mice From Hepatic Ischemia/Reperfusion Injury

Mathieu Panel, Isaac Ruiz, Rozenn Brillet, Fouad Lafdil, Fatima Teixeira-Clerc, Cong Trung Nguyen, Julien Caldéraro, Muriel Gelin, Fred Allemand, Jean-François Guichou, et al.

### ► To cite this version:

Mathieu Panel, Isaac Ruiz, Rozenn Brillet, Fouad Lafdil, Fatima Teixeira-Clerc, et al.. Small-Molecule Inhibitors of Cyclophilins Block Opening of the Mitochondrial Permeability Transition Pore and Protect Mice From Hepatic Ischemia/Reperfusion Injury. *Gastroenterology*, 2019, 157 (5), pp.1368-1382. 10.1053/j.gastro.2019.07.026 . hal-02391962

**HAL Id: hal-02391962**

**<https://hal.science/hal-02391962>**

Submitted on 24 Nov 2020

**HAL** is a multi-disciplinary open access archive for the deposit and dissemination of scientific research documents, whether they are published or not. The documents may come from teaching and research institutions in France or abroad, or from public or private research centers.

L'archive ouverte pluridisciplinaire **HAL**, est destinée au dépôt et à la diffusion de documents scientifiques de niveau recherche, publiés ou non, émanant des établissements d'enseignement et de recherche français ou étrangers, des laboratoires publics ou privés.

1 **Small-molecule inhibitors of cyclophilins block opening of the mitochondrial**  
2 **permeability transition pore and protect mice from hepatic ischemia–reperfusion injury**

3  
4 Mathieu Panel,<sup>1,2\*</sup> Isaac Ruiz,<sup>3\*</sup> Rozenn Brilllet,<sup>3</sup> Fouad Lafdil,<sup>3,4</sup> Fatima Teixeira-Clerc,<sup>3</sup>  
5 Cong Trung Nguyen,<sup>3,5</sup> Julien Calderaro,<sup>3,5</sup> Muriel Gelin,<sup>6</sup> Fred Allemand,<sup>6</sup> Jean-François  
6 Guichou,<sup>6</sup> Bijan Ghaleh,<sup>1,2</sup> Abdelhakim Ahmed-Belkacem,<sup>3#</sup> Didier Morin,<sup>1,2#</sup>  
7 and Jean-Michel Pawlotsky<sup>3,7#</sup>  
8  
9

10 <sup>1</sup>INSERM U955, Team 3, Créteil, France; <sup>2</sup>Université Paris-Est, UMR S955, DHU A-TVB,  
11 UPEC, Créteil, France; <sup>3</sup>INSERM U955, Team “Pathophysiology and Therapy of Chronic  
12 Viral Hepatitis and Related Cancers“, Créteil, France; <sup>4</sup>Institut Universitaire de France (IUF),  
13 Paris, France; <sup>5</sup>Department of Pathology, Hôpital Henri Mondor, Université Paris-Est, Créteil,  
14 France; <sup>6</sup>Centre de Biochimie Structurale (CBS), INSERM U1054, CNRS UMR5048,  
15 Université de Montpellier, Montpellier, France; <sup>7</sup>National Reference Center for Viral  
16 Hepatitis B, C and Delta, Department of Virology, Hôpital Henri Mondor, Université Paris-  
17 Est, Créteil, France  
18

19 **Abstract**

20 **Background & Aims:** Hepatic ischemia–reperfusion injury is a complication of liver  
21 surgery that involves mitochondrial dysfunction resulting from mitochondrial permeability  
22 transition pore (mPTP) opening. Cyclophilin D (PPIF or CypD) is a peptidyl-prolyl cis-trans  
23 isomerase that regulates mPTP opening in the inner mitochondrial membrane. We investigated  
24 whether and how recently created small-molecule inhibitors of CypD prevent opening of the  
25 mPTP in hepatocytes and the resulting effects in cell models and livers of mice undergoing  
26 ischemia–reperfusion injury.

27 **Methods:** We measured the activity of 9 small-molecule inhibitors of Cyps in an assay  
28 of CypD activity. The effects of the small-molecule CypD inhibitors or vehicle on mPTP  
29 opening were assessed by measuring mitochondrial swelling and calcium retention in isolated  
30 liver mitochondria from C57BL/6J (wild-type) and *Ppif*<sup>-/-</sup> (CypD knock-out) mice, and in  
31 primary mouse and human hepatocytes by fluorescence microscopy. We induced ischemia–  
32 reperfusion injury in livers of mice given a small-molecule CypD inhibitor or vehicle before  
33 and during reperfusion, and collected samples of blood and liver for histologic analysis.

34 **Results:** The compounds inhibited peptidyl-prolyl isomerase activity (IC<sub>50</sub> values, 0.2  
35 to 16.2 μM) and, as a result, calcium-induced mitochondrial swelling, by preventing mPTP  
36 opening (IC<sub>50</sub> values, 1.4 to 132 μM) in a concentration-dependent manner. The most potent  
37 inhibitor (C31) bound CypD with high affinity and inhibited swelling in mitochondria from  
38 livers of wild-type and *Ppif*<sup>-/-</sup> mice (indicating an additional, CypD-independent effect on  
39 mPTP opening) and in primary human and mouse hepatocytes. Administration of C31 in mice  
40 with ischemia–reperfusion injury before and during reperfusion restored hepatic calcium  
41 retention capacity and oxidative phosphorylation parameters and reduced liver damage  
42 compared with vehicle.  
43

44 **KEY WORDS:** drug, mitochondrial swelling, PPIase activity, mouse model.  
45

46 **doi: 10.1053/j.gastro.2019.07.026.**  
47

48 **Small-molecule inhibitors of cyclophilins block opening of the mitochondrial**  
 49 **permeability transition pore and protect mice from hepatic ischemia–reperfusion injury**

50

51 Mathieu Panel,<sup>1,2\*</sup> Isaac Ruiz,<sup>3\*</sup> Rozenn Brilllet,<sup>3</sup> Fouad Lafdil,<sup>3,4</sup> Fatima Teixeira-Clerc,<sup>3</sup>  
 52 Cong Trung Nguyen,<sup>3,5</sup> Julien Calderaro,<sup>3,5</sup> Muriel Gelin,<sup>6</sup> Fred Allemand,<sup>6</sup> Jean-François  
 53 Guichou,<sup>6</sup> Bijan Ghaleh,<sup>1,2</sup> Abdelhakim Ahmed-Belkacem,<sup>3#</sup> Didier Morin,<sup>1,2#</sup>  
 54 and Jean-Michel Pawlotsky<sup>3,7#</sup>

55

56 \*Authors share co-first authorship

57 #Authors share co-senior authorship.

58

59 <sup>1</sup>INSERM U955, Team 3, Créteil, France; <sup>2</sup>Université Paris-Est, UMR S955, DHU A-TVB,  
 60 UPEC, Créteil, France; <sup>3</sup>INSERM U955, Team “Pathophysiology and Therapy of Chronic  
 61 Viral Hepatitis and Related Cancers“, Créteil, France; <sup>4</sup>Institut Universitaire de France (IUF),  
 62 Paris, France; <sup>5</sup>Department of Pathology, Hôpital Henri Mondor, Université Paris-Est, Créteil,  
 63 France; <sup>6</sup>Centre de Biochimie Structurale (CBS), INSERM U1054, CNRS UMR5048,  
 64 Université de Montpellier, Montpellier, France; <sup>7</sup>National Reference Center for Viral  
 65 Hepatitis B, C and Delta, Department of Virology, Hôpital Henri Mondor, Université Paris-  
 66 Est, Créteil, France

67

68 **SHORT TITLE: Cyclophilin inhibition and hepatic ischemia-reperfusion**

69

70 **Corresponding authors:**

71 - **Jean-Michel Pawlotsky** :Department of Virology, Hôpital Henri Mondor, 51 avenue  
 72 du Maréchal de Lattre de Tassigny, 94010 Créteil, France.

73 E-mail : [jean-michel.pawlotsky@aphp.fr](mailto:jean-michel.pawlotsky@aphp.fr)

74 - **Didier Morin** : INSERM U955, équipe 3, Faculté de Médecine, 8 rue du général Sarrail,  
75 94000, Créteil, France.

76 E-mail : didier.morin@inserm.fr

77

78 **Grant support:** Mathieu Panel was supported by a grant from the French Ministry for Higher  
79 Education and Research (Grant #2014-140). Isaac Ruiz was supported by grants from the  
80 National Agency for Research on AIDS and Viral Hepatitis (ANRS) and the Mexican National  
81 Council of Science and Technology (CONACYT).

82

83 **Conflict of interest disclosures:** Inserm Transfert is the owner of patent EP 09306294.1  
84 covering the family of cyclophilin inhibitors described, for which Abdelhakim Ahmed-  
85 Belkacem, Jean-François Guichou and Jean-Michel Pawlotsky are inventors. All other authors  
86 declare no competing financial interests.

87

88 **Acknowledgement:** The authors are grateful to Drs Joseph Benga and Stéphane Moutereau  
89 from the Department of Biochemistry at Henri Mondor hospital for ALT and AST level  
90 measurements and to Prof. René Tolba and Dr Zoltan Czigany from the Aachen University  
91 Hospital, Germany, for helpful discussions regarding the *in vivo* ischemia-reperfusion injury  
92 model.

93

94 **Authors contributions:**

95 - Mathieu Panel: acquisition, analysis and interpretation of data; drafting of the  
96 manuscript; statistical analysis.

97 - Isaac Ruiz: contribution to the experimental design of murine ischemia-reperfusion  
98 experiments; acquisition, analysis and interpretation of data.

99 - Rozenn Brillet: acquisition, analysis and interpretation of data.

- 100 - Fouad Lafdil: contribution to the experimental design of murine ischemia-reperfusion  
101 experiments; revision of the manuscript.
- 102 - Fatima Teixeira-Clerc: contribution to the experimental design of murine ischemia-  
103 reperfusion experiments; revision of the manuscript.
- 104 - Cong Trung Nguyen: acquisition, analysis and interpretation of histological data.
- 105 - Julien Calderaro: acquisition, analysis and interpretation of histological data.
- 106 - Muriel Gelin: acquisition, analysis and interpretation of chemical data.
- 107 - Fred Allemand: acquisition, analysis and interpretation of chemical data.
- 108 - Jean-François Guichou: compound design and synthesis; generation of structural data;  
109 revision of the manuscript.
- 110 - Bijan Ghaleh: study supervision; analysis and interpretation of data; drafting of the  
111 manuscript.
- 112 - Abdelhakim Ahmed-Belkacem: study supervision; acquisition, analysis and  
113 interpretation of data; drafting of the manuscript.
- 114 - Didier Morin: study supervision; analysis and interpretation of data; drafting of the  
115 manuscript.
- 116 - Jean-Michel Pawlotsky: study supervision; analysis and interpretation of data; critical  
117 revision of the manuscript for important intellectual content.
- 118

119 **Abstract**

120

121 **Background & Aims:** Hepatic ischemia–reperfusion injury is a complication of liver  
122 surgery that involves mitochondrial dysfunction resulting from mitochondrial permeability  
123 transition pore (mPTP) opening. Cyclophilin D (PPIF or CypD) is a peptidyl-prolyl cis-trans  
124 isomerase that regulates mPTP opening in the inner mitochondrial membrane. We investigated  
125 whether and how recently created small-molecule inhibitors of CypD prevent opening of the  
126 mPTP in hepatocytes and the resulting effects in cell models and livers of mice undergoing  
127 ischemia–reperfusion injury.

128 **Methods:** We measured the activity of 9 small-molecule inhibitors of CyPs in an assay  
129 of CypD activity. The effects of the small-molecule CypD inhibitors or vehicle on mPTP  
130 opening were assessed by measuring mitochondrial swelling and calcium retention in isolated  
131 liver mitochondria from C57BL/6J (wild-type) and *Ppif*<sup>-/-</sup> (CypD knock-out) mice, and in  
132 primary mouse and human hepatocytes by fluorescence microscopy. We induced ischemia–  
133 reperfusion injury in livers of mice given a small-molecule CypD inhibitor or vehicle before  
134 and during reperfusion, and collected samples of blood and liver for histologic analysis.

135 **Results:** The compounds inhibited peptidyl-prolyl isomerase activity (IC<sub>50</sub> values, 0.2  
136 to 16.2 μM) and, as a result, calcium-induced mitochondrial swelling, by preventing mPTP  
137 opening (IC<sub>50</sub> values, 1.4 to 132 μM) in a concentration-dependent manner. The most potent  
138 inhibitor (C31) bound CypD with high affinity and inhibited swelling in mitochondria from  
139 livers of wild-type and *Ppif*<sup>-/-</sup> mice (indicating an additional, CypD-independent effect on  
140 mPTP opening) and in primary human and mouse hepatocytes. Administration of C31 in mice  
141 with ischemia–reperfusion injury before and during reperfusion restored hepatic calcium  
142 retention capacity and oxidative phosphorylation parameters and reduced liver damage  
143 compared with vehicle.

144           **Conclusions:** Recently created small-molecule inhibitors of CypD reduced calcium-  
145 induced swelling in mitochondria from mouse and human liver tissues. Administration of these  
146 compounds to mice during ischemia–reperfusion restored hepatic calcium retention capacity  
147 and oxidative phosphorylation parameters and reduced liver damage. These compounds might  
148 be developed to protect patients from ischemia–reperfusion injury after liver surgery or for  
149 other hepatic or non-hepatic disorders related to abnormal mPTP opening.

150

151 **KEY WORDS:** drug, mitochondrial swelling, PPIase activity, mouse model.

152

## 153 **Introduction**

154

155           Hepatic ischemia-reperfusion injury is a major complication of liver surgery, including  
156 liver resection, liver transplantation, and trauma surgery<sup>1</sup>. Ischemia results from the interruption  
157 of the blood flow that perturbs the cellular metabolism as a result of oxygen shortage.  
158 Reperfusion restores the blood flow, oxygen delivery and tissue pH, thereby exacerbating  
159 cellular damage initiated during hypoxia or anoxia<sup>2, 3</sup>. Hepatic ischemia-reperfusion injury is  
160 an important cause of liver dysfunction or functional failure post-liver surgery, which affects  
161 perioperative morbidity, mortality and recovery<sup>2, 3</sup>. There are two types of ischemia: the most  
162 frequent form, warm ischemia, is observed when vascular occlusion occurs during hepatic  
163 resection surgery or during exposure to low-flow incidences such as trauma, hemorrhagic  
164 shock, cardiac arrest or hepatic sinusoidal obstruction syndrome; cold ischemia is observed  
165 exclusively during orthotopic liver transplantation, when the graft is subjected to hypothermic  
166 preservation before warm reperfusion<sup>3</sup>. Their mechanisms and main target cells differ.  
167 Hepatocytes are a major target of warm ischemia-reperfusion injury through anoxia, nutrition  
168 depletion and cytosolic acidosis<sup>3</sup>. In particular, sodium, chloride and calcium homeostasis are  
169 significantly altered.

170           Mitochondrial dysfunction plays a major role in hepatic ischemia-reperfusion injury<sup>3</sup>.  
171 Indeed, ischemia-reperfusion triggers the mitochondrial permeability transition, characterized  
172 by an increase in the permeability of the inner mitochondrial membrane mediated by the  
173 opening of a channel, called the “mitochondrial permeability transition pore“ (mPTP)<sup>4</sup>. Once  
174 mitochondrial permeability transition initiates, solutes with a molecular mass of up to 1.5 kDa  
175 diffuse across the mitochondrial inner membrane, inducing mitochondrial depolarization,  
176 uncoupling and swelling, which in turn induce ATP depletion and necrotic (and, to a lesser  
177 extent, apoptotic) cell death<sup>3</sup>. During hepatic ischemia-reperfusion, mPTP opening is triggered  
178 by calcium-mediated mitochondrial reactive oxygen species formation. The same phenomenon

179 has been reported to play an important role during ischemia-reperfusion affecting other organs  
180 (including heart and brain)<sup>5-8</sup>, neurodegenerative diseases<sup>9</sup> and drug-induced liver injury<sup>10</sup>.

181 Therapies avoiding the consequences of hepatic ischemia-reperfusion injury remain  
182 limited. Given the key role of mPTP opening in ischemia-reperfusion injury, pharmacological  
183 inhibition of mPTP opening is a promising target for new therapies. However, the molecular  
184 structure and functioning of mPTP remain largely unknown. Several proteins have been  
185 suggested to be involved in the structure of mPTP, including ATP synthase, the adenine  
186 nucleotide translocase, a phosphate carrier, and cyclophilin D (CypD)<sup>11</sup>. Cyclophilins are  
187 peptidyl prolyl *cis/trans* isomerases (PPIases) that catalyze the interconversion of the two  
188 energetically preferred conformers (*cis* and *trans*) of the planar peptide bond preceding an  
189 internal proline residue. Seventeen human cyclophilins have been identified, but the function  
190 of most of them is unknown<sup>12,13</sup>. CypD is located within the mitochondrial matrix where it acts  
191 as a key component and regulator of the mPTP; mPTP formation appears to be catalyzed or  
192 stabilized by CypD through lowering of its calcium threshold<sup>14</sup>. Thus, CypD represents an  
193 attractive target for mPTP opening inhibition and cellular protection in the context of hepatic  
194 ischemia-reperfusion injury.

195 Cyclosporine A (CsA) and its derivatives (together with sanglifehrin A) are known  
196 macromolecular CypD ligands. They have been shown to efficiently desensitize mPTP opening  
197 in various cellular and *in vivo* models<sup>15-18</sup>. However, CsA is a potent immunosuppressor and its  
198 non-immunosuppressive derivatives suffer from many disadvantages, including their size,  
199 complex multistep synthesis, cell toxicity and lack of chemical plasticity. Thus, potent  
200 cyclophilin inhibitors unrelated to CsA or sanglifehrin A and lacking the disadvantages of non-  
201 immunosuppressive macromolecular CsA derivatives are needed.

202 By means of a fragment-based drug discovery approach based on X-ray crystallography  
203 and nuclear magnetic resonance, we generated a new family of nonpeptidic small-molecule  
204 cyclophilin inhibitors (SMCypIs) unrelated to CsA or sanglifehrin A, with potent inhibitory

205 activity against CypA, CypB and CypD<sup>19</sup>. These compounds lack cellular toxicity and  
206 immunosuppressive activity and bear druggable pharmacological properties<sup>19</sup>. In this study, we  
207 assessed the ability of the new SMCypIs to inhibit liver mitochondria mPTP opening through  
208 CypD inhibition, studied their mechanisms of inhibition, and evaluated *in vivo* their protective  
209 properties in the context of experimental hepatic ischemia-reperfusion injury.

210

## 211 **Materials and Methods**

212

### 213 *Drugs and cells*

214

215 Unless specified, all reagents were purchased from Sigma-Aldrich (Saint-Quentin  
216 Fallavier, France). Calcein AM (C3100MP) and calcium Green 5N (C3737) were obtained from  
217 Invitrogen (Cergy-Pontoise, France). SMCypIs were synthesized as previously described<sup>19</sup>.  
218 Primary human hepatocytes were obtained from Biopredict International (Saint-Grégoire,  
219 France).

220

### 221 *Animals*

222

223 Male C57BL/6J mice (8 to 10-week-old) were purchased from Janvier (Le Genest-St-  
224 Isle, France). *Ppif*<sup>-/-</sup> mice (i.e., CypD knock-out mice) were obtained from Jackson Laboratories  
225 (Bar Harbor, Maine). Animals were co-housed in an air-conditioned room with a 12-h light-  
226 dark cycle and received standard rodent chow and drinking water *ad libitum*. All animal  
227 procedures in this study were in strict accordance with the Directives of the European  
228 Parliament (2010/63/EU-848 EEC) and approved by the Animal Ethics Committee  
229 ANSES/ENVA/Université Paris-Est Créteil (approval numbers 09/12/14-02 and 11/10/16-01).

230

### 231 ***Molecular modeling and docking of C31 into CypD***

232

233 Molecular modeling and docking experiments were performed by means of the  
234 @TOME-2 server<sup>20</sup>. In each structural model, the boundaries of the active site were deduced  
235 from the vicinity of co-crystallized ligands (compounds C30, C27, and C24 selected as  
236 templates, with PDB accession numbers 4J5C, 4J5B and 4J5E, respectively) using @TOME-2  
237 comparative option. They were used to guide docking in automatically computed models. The  
238 ligand files were generated with MarvinSketch 6.2.2 for SMILES and Frog2 server for mol2<sup>21</sup>.  
239 The Figure was generated by means of Pymol.

240

### 241 ***CypD PPIase enzyme assay***

242

243 Inhibition of CypD PPIase activity was measured at 20°C by means of the standard  
244 chymotrypsin coupled assay. The assay buffer (25 mM HEPES, 100 mM NaCl, pH 7.8) and  
245 purified CypD (1900 nM stock solution) were pre-cooled at 4°C in the presence of serial  
246 dilutions of the SMCypIs. Five µL of 50 mg/mL chymotrypsin in 1 mM HCl was added. The  
247 reaction was initiated by adding 20 µL of 3.2 mM peptide substrate (N-succinyl-Ala-Ala-Cis-  
248 Pro-Phe-p-nitroanilide). P-nitroanilide absorbance was measured at 390 nm for 1 min. CsA was  
249 used as a positive control of PPIase inhibition. The percent inhibition of CypD PPIase activity  
250 was calculated from the slopes and the IC<sub>50s</sub> were determined from percent inhibition curves  
251 using Sigmaplot software.

252

### 253 ***Isolation of liver mitochondria***

254

255 Mouse livers were scissor-minced and homogenized on ice in a buffer (220 mM  
256 mannitol, 70 mM sucrose, 10 mM HEPES, 4 mM EGTA, pH 7.4 at 4°C) using a Potter-

257 Elvehjem glass homogenizer in a final volume of 10 mL. The homogenate was centrifuged at  
258 1000 g for 5 min at 4°C. The supernatant was centrifuged at 10,000 g for 10 min at 4°C. The  
259 mitochondrial pellet was resuspended in 600 µl of homogenization buffer without EGTA and  
260 protein concentration was determined.

261

### 262 *Measurement of mitochondrial oxygen consumption*

263

264 Oxygen consumption of isolated mitochondria was measured with a Clark-type  
265 electrode fitted to a water-jacketed reaction chamber (Hansatech, Cergy, France). Mitochondria  
266 (1 mg protein/mL) were incubated at 30°C in a respiration buffer containing 100 mM KCl, 50  
267 mM sucrose, 10 mM HEPES and 5 mM KH<sub>2</sub>PO<sub>4</sub> at pH 7.4. Respiration was initiated by the  
268 addition of glutamate/malate (5 mM each). After 1 min, ATP synthesis was induced by the  
269 addition of 1 mM ADP (state 3 respiration rate), and 1 µM carboxyatractyloside was added to  
270 measure the substrate-dependent respiration rate (state 4). The respiratory control ratio (state  
271 3/state 4) was then calculated.

272

### 273 *Mitochondrial swelling assays*

274

275 Mitochondrial swelling was assessed by measuring the change in absorbance at 540 nm  
276 (A<sub>540</sub>) using a Jasco V-530 spectrophotometer equipped with magnetic stirring and thermostatic  
277 control. Mitochondria (0.5 mg/mL) energized with pyruvate/malate (5 mM each) were  
278 incubated 30 sec in the respiration buffer before the induction of swelling with 10 mM  
279 phosphate, 100 µM atractyloside or 40 µM *tert*-butyl hydroperoxide in the presence of 50 µM  
280 of CaCl<sub>2</sub>.

281 In de-energized conditions, mitochondria (0.5 mg/mL) were incubated 1 min at 30°C in  
282 a swelling buffer containing 100 mM KCl, 50 mM sucrose, 10 mM HEPES, 5 mM KH<sub>2</sub>PO<sub>4</sub>, 1

283  $\mu\text{M}$  rotenone, and 1  $\mu\text{M}$  antimycin at pH 7.4. Then, 50  $\mu\text{M}$  or 100  $\mu\text{M}$   $\text{CaCl}_2$  was added 1 min  
284 before swelling induction with 1  $\mu\text{M}$  of A23187 or 10  $\mu\text{M}$  phenylarsine oxide, respectively.

285 In both conditions, SMCypIs or CsA were introduced at the beginning of the incubation  
286 period.

287

### 288 *Measurement of the calcium retention capacity of isolated mitochondria*

289

290 Mitochondria were loaded with increasing concentrations of calcium until mPTP  
291 opening and fast calcium release occurred<sup>22</sup>. Liver mitochondria (1 mg/mL) energized with 5  
292 mM glutamate/malate were incubated in the respiration buffer supplemented with 1  $\mu\text{M}$   
293 Calcium Green-5N fluorescent probe. The calcium concentration in the extra-mitochondrial  
294 medium was monitored by means of a Jasco FP-6300 spectrofluorimeter (Jasco, Bouguenais,  
295 France) at excitation and emission wavelengths of 506 and 532 nm, respectively. The calcium  
296 signal was calibrated by addition of known calcium amounts to the medium.

297

### 298 *Isolation of primary mouse hepatocytes*

299

300 Murine hepatocytes from C57BL6 animals were isolated by portal vein perfusion of  
301 collagenase<sup>23</sup>. Freshly isolated hepatocytes were cultured in DMEM supplemented with 10%  
302 fetal calf serum, 10 U/mL penicillin, 10  $\mu\text{g}/\text{mL}$  streptomycin, 10  $\mu\text{g}/\text{mL}$  insulin, 5.5  $\mu\text{g}/\text{mL}$   
303 transferrin and 5 ng/mL sodium selenite. Four hours post-perfusion, the medium was removed  
304 and fresh medium, supplemented with 0.1  $\mu\text{M}$  dexamethasone and 50 ng/mL epidermal growth  
305 factor, was added.

306

### 307 *Measurement of mPTP opening in primary mouse and human hepatocytes*

308

309 mPTP opening was assessed in primary mouse and human hepatocytes by inducing  
310 mitochondrial localization of calcein fluorescence<sup>24</sup>. Cells were loaded with 2 mM CoCl<sub>2</sub> at  
311 30°C in 1 mL of Tyrode's solution (NaCl 130 mM, KCl 5 mM, HEPES 10 mM, MgCl<sub>2</sub> 1 mM,  
312 CaCl<sub>2</sub> 1.8 mM, pH 7.4 at 37°C) for 30 min. After 10 min, the cells were supplemented with 1  
313 μM calcein acetoxymethyl ester, washed free of calcein and CoCl<sub>2</sub>, placed in a thermostated  
314 chamber and incubated in Tyrode's solution. After 5 min, 2 μM of calcium ionophore A23187  
315 was added to induce mPTP opening<sup>25</sup>. When specified, either C31 or CsA was added at the  
316 beginning of the incubation period.

317 Cells were imaged with an Olympus IX-81 motorized inverted microscope equipped  
318 with a mercury lamp as the light source for epifluorescence illumination, combined with a 12-  
319 bit cooled Hamamatsu ORCA-ER camera; 460-490 nm excitation and 510 nm emission filters  
320 were used for detection of calcein fluorescence. Images were acquired every min for 30 min  
321 after 30 ms of illumination per image using a digital epifluorescence imaging software (Cell M,  
322 Olympus, Rungis, France). Fluorescence from each cell in each region of interest ( $\approx 80 \mu\text{m}^2$ )  
323 was measured and background fluorescence was subtracted. Average fluorescence changes per  
324 field were calculated. Fluorescence was normalized to the maximal fluorescence value.

325

### 326 *Ex vivo assessment of mPTP opening in mice treated with C31*

327

328 The mice were anesthetized by intraperitoneal injection of pentobarbital sodium (80  
329 mg/kg). Increasing doses of C31 (10, 20, 50 and 150 mg/kg) or vehicle were randomly  
330 administered as a 3-min infusion through the jugular vein. Two min after the end of the infusion,  
331 the livers were excised and mitochondria were isolated to measure their capacity to retain  
332 calcium, as a marker of the ability of C31 to inhibit mPTP opening *in vivo*.

333

334 ***In vivo assessment of the mito- and hepatoprotective effect of SMCypIs in the context of***  
335 ***hepatic ischemia-reperfusion***

336

337 The mice were anesthetized by intraperitoneal injection of pentobarbital sodium (80  
338 mg/kg), intubated and mechanically ventilated. After section of the liver ligaments, hepatic  
339 normothermic ischemia of segments I to V was induced for 60 min by hilum clamping of the  
340 hepatic pedicle. Reperfusion occurred at removal of the clamp. One min before reperfusion,  
341 C31 or the vehicle was infused through the jugular vein and the infusion was maintained for  
342 the first 8 min of reperfusion.

343 Two sets of experiments were conducted. In the first set, livers were excised after 10  
344 min of reperfusion and mitochondria were isolated for *ex vivo* experiments. In the second set,  
345 reperfusion was stopped after 60 min; 500  $\mu$ L of blood was collected to measure alanine  
346 aminotransferase (ALT) and aspartate aminotransferase (AST) levels, while livers were  
347 excised, formalin-fixed, paraffin-embedded and liver sections were stained with hematoxylin  
348 and eosin. “Hepatocyte clarification”, a histological feature of severe hepatocellular damage  
349 characterized by hepatocyte ballooning degeneration, was measured on whole sections of mice  
350 livers. Histological slides were scanned at an x20 magnification by means of an Aperio Slide  
351 Scanner (Leica Biosystems, Shanghai, China). Slides in “.svs” format were analyzed by means  
352 of Qupath open source software<sup>26</sup>. Areas with hepatocyte ballooning were then manually  
353 annotated independently by two pathologists specialized in liver diseases.

354

355 ***Statistical analysis***

356

357 Results are expressed as mean $\pm$ SEM of at least 5 independent experiments. Statistical  
358 analysis was performed using one-way ANOVA followed by the Scheffé *post-hoc* test.  
359 Differences were considered significant for  $p < 0.05$ .

360

361 **Results**

362

363 *SMCypIs bind CypD and inhibit its PPIase activity*

364

365 We recently created a new family of small-molecule, nonpeptidic cyclophilin inhibitors  
366 (SMCypI)<sup>19</sup>. As shown in Supplementary Table 1 and Supplementary Figure 1, 9 members of  
367 the new SMCypI family, including compound C22, compounds C23 to C27 and compounds  
368 C29 to C31 (which all resulted from structure-guided chemical optimization of C22), inhibited  
369 CypD PPIase activity in an enzyme assay, with IC<sub>50</sub> values ranging from 0.2 to 16.2 μM. The  
370 most potent PPIase inhibitor was C31, with an IC<sub>50</sub> of 0.2±0.08 μM. Molecular modeling and  
371 docking experiments revealed that C31 binds both the catalytic site and the gatekeeper pocket  
372 of CypD (Figure 1A).

373

374 *SMCypIs inhibit calcium-induced swelling as a result of the inhibition of CypD PPIase*  
375 *activity in isolated mouse liver mitochondria*

376

377 As shown in Figure 1B, 1 μM CsA, used as a positive control of CypD inhibition, fully  
378 inhibited calcium-induced swelling of energized isolated mouse liver mitochondria. The 9  
379 SMCypIs also inhibited mitochondrial swelling in a concentration-dependent manner  
380 (Supplementary Table 1). The most effective compound was C31, with an IC<sub>50</sub> of 1.4±0.2 μM  
381 (Figure 1B). SMCypI inhibition of calcium-induced mitochondrial swelling strongly correlated  
382 with SMCypI inhibition of CypD PPIase activity ( $r=0.8535$ ;  $p < 0.004$ ; Figure 1C).

383 These results indicate that the new SMCypI family inhibits calcium-induced  
384 mitochondrial swelling as a result of CypD PPIase activity inhibition by binding to both the

385 PPIase catalytic site and the gatekeeper pocket of CypD. C31, the most potent SMCypI, was  
386 selected for subsequent experiments.

387

388 ***SMCypI inhibition of mitochondrial swelling is due to the inhibition of mPTP opening***

389

390 To assess whether mitochondrial swelling inhibition by SMCypIs is related to the  
391 inhibition of mPTP opening, swelling was induced by different known mPTP opening inducers.  
392 As shown in Figures 2A and 2B, C31 inhibited mitochondrial swelling induced by both the pro-  
393 oxidant drug *tert*-butyl hydroperoxide and carboxyatractyloside, a ligand of adenine nucleotide  
394 translocase, in energized conditions.

395 Because mitochondrial parameters, such as the membrane potential or the ATP/ADP  
396 ratio, can modulate mPTP opening under energized conditions, thereby influencing the  
397 observed effect of the inhibitors, the inhibitory effect of C31 was analyzed under de-energized  
398 conditions, i.e., in the absence of substrate. Mitochondria were incubated in the presence of  
399 rotenone and antimycin to fully block the respiratory chain and supplemented with the calcium  
400 ionophore A23187 or the cross-linking thiol agent phenylarsine oxide in the presence of  
401 calcium. In these conditions (Figure 2C and 2D, respectively), mitochondrial swelling was  
402 slower than under energized conditions, but still inhibited by SMCypI C31.

403 These results indicate that SMCypI compound C31 inhibits mitochondrial swelling by  
404 inhibiting mPTP opening.

405

406 ***SMCypI compound C31 inhibits mPTP opening in both primary mouse and human***  
407 ***hepatocytes***

408

409 Primary mouse hepatocytes were loaded with calcein in the presence of CoCl<sub>2</sub> and  
410 mPTP opening was induced by the addition of 1μM A23187 (Figure 3A). As shown in Figure

411 3B, CsA inhibited the drop in calcein fluorescence associated with mPTP opening by only  
412  $55.4\pm 0.8\%$  at 30 min at the most effective concentration of  $2\ \mu\text{M}$ . C31 inhibited the drop in  
413 calcein fluorescence in a concentration-dependent manner, a result indicating that C31 inhibits  
414 mPTP opening in living mouse liver cells (Figure 3B). The inhibitory effect of C31 was stronger  
415 than that of  $2\ \mu\text{M}$  CsA, with full inhibition of mPTP opening obtained with  $100\ \mu\text{M}$  of C31.

416 The same experiments were performed with primary human hepatocytes (Figure 3C).  
417 CsA inhibited mPTP opening by approximately 50% at the most effective concentration of  $0.2\ \mu\text{M}$ .  
418 C31 inhibited mPTP opening in a concentration-dependent manner in primary human  
419 hepatocytes, with full inhibition achieved at the concentration of  $100\ \mu\text{M}$  (Figure 3C). This  
420 indicated that results obtained in mouse liver cells are representative of the human liver  
421 situation.

422

423 ***SMCypI compound C31 is more potent than CsA at increasing mitochondrial calcium***  
424 ***retention capacity in isolated mouse mitochondria***

425

426 The calcium retention capacity of isolated mouse mitochondria (i.e., the maximal  
427 calcium load achievable in the presence of a drug before mPTP opens) was measured, as  
428 previously described<sup>22</sup>. As shown in Figures 4A and 4B,  $6\pm 1$  additions of  $20\ \mu\text{M}$  calcium,  
429 corresponding to  $109\pm 15$  nmol/mg of mitochondrial proteins, were required to induce mPTP  
430 opening in the absence of CypD inhibitors. One  $\mu\text{M}$  of CsA increased the mitochondrial  
431 calcium retention capacity by 3-fold ( $337\pm 47$  nmol/mg of mitochondrial proteins). C31 at  
432 concentrations up to  $100\ \mu\text{M}$  also increased the mitochondrial calcium retention capacity. The  
433 maximum effect of C31 was markedly greater than that of CsA ( $550\pm 37$  nmol/mg of  
434 mitochondrial proteins; Figures 4A and 4B). C31 also more potently increased mitochondrial  
435 calcium retention capacity than CsA when the respiratory chain was fed with succinate in the

436 presence of rotenone, indicating that this effect is independent from activated respiratory  
437 complex I or II (data not shown).

438 Maximum mitochondrial calcium retention capacities of the same order were achieved  
439 in the presence of 10  $\mu\text{M}$  of C31 and 1  $\mu\text{M}$  of CsA, respectively. At these concentrations, that  
440 correspond to approximately 10 times the respective compound  $\text{IC}_{50}$  values, CypD saturation  
441 is achieved. The combination of both C31 and CsA at the same concentrations did not result in  
442 any additive effect (Figure 4B), a result in keeping with them sharing CypD as a target.

443 Together, these results indicate that SMCypI compound C31 inhibits mPTP opening at  
444 least partly through CypD inhibition, and that this inhibition is more potent than that achieved  
445 by CsA.

446

447 *The additional effectiveness of C31 as compared to CsA in inhibiting mPTP opening is*  
448 *unrelated to CypD inhibition*

449

450 The mitochondrial calcium retention capacity in the presence of 100  $\mu\text{M}$  C31 was not  
451 modified by the addition of 1  $\mu\text{M}$  CsA (Figure 4B). This suggests that the greater capacity of  
452 C31 to inhibit mPTP opening as compared to CsA is unrelated to CypD inhibition. To verify  
453 this hypothesis, the effects of C31 and CsA were assessed on liver mitochondria isolated from  
454 *Ppif*<sup>-/-</sup> mice, which have been knocked-out for CypD, in comparison with wild-type animals.  
455 As previously shown<sup>27</sup>, the mitochondrial calcium retention capacity of *Ppif*<sup>-/-</sup> mice was  
456 approximately 4-fold greater than that of wild-type animals (Figure 5A and 5B). CsA 1  $\mu\text{M}$  had  
457 no effect on *Ppif*<sup>-/-</sup> mice mitochondrial calcium retention capacity. In contrast, C31 increased  
458 the calcium retention capacity by approximately 1.5-fold at concentrations  $>20$   $\mu\text{M}$  in  
459 mitochondria isolated from *Ppif*<sup>-/-</sup> mice livers (Figure 5A and 5B). The C31 concentrations at  
460 which this effect was observed were higher than those required to inhibit CypD PPIase activity  
461 and mitochondrial swelling and to enhance calcium retention capacity in wild-type mouse

462 mitochondria (see Figures 1 and 3 for comparison). In addition, C31 inhibited swelling induced  
463 by very high calcium concentrations in mitochondria isolated from *Ppif*<sup>-/-</sup> mice (Figure 5C).

464 These results indicate that, in addition to blocking CypD, C31 interacts with another  
465 target at the mPTP level and that this interaction increases C31 blocking effectiveness on mPTP  
466 opening as compared to exclusive CypD inhibitors, such as CsA.

467

468 *The additional effectiveness of C31 as compared to CsA in inhibiting mPTP opening is*  
469 *related to the chemical structure of its phenyl moiety*

470

471 Comparison of the chemical structures of the SMCypIs (Supplementary Figure 1)  
472 suggested that the phenyl moiety of C31 is involved in this additional effect: indeed, SMCypI  
473 compound C34, that lacks the aromaticity of the cycle, lost the additional effect of C31 over  
474 CypD inhibition in isolated *Ppif*<sup>-/-</sup> mouse liver mitochondria shown in Figure 5D.

475

476 *The additional effectiveness of C31 as compared to CsA in inhibiting mPTP opening is*  
477 *unrelated to a ubiquinone-like effect or an interaction with the mitochondrial respiratory*  
478 *chain.*

479

480 Ubiquinones have been shown to inhibit mPTP opening to a greater extent than CsA<sup>28</sup>.  
481 The proximity between the urea and phenyl motifs of C31 would be compatible with a shared  
482 mPTP target with ubiquinones. As shown in Figure 5E, ubiquinone 0 (Ub<sub>0</sub>), the most efficient  
483 ubiquinone, strongly increased the calcium retention capacity of liver mitochondria isolated  
484 from wild-type mice, but had no effect in liver mitochondria isolated from *Ppif*<sup>-/-</sup> mice (Figure  
485 5E). This result indicates that the additional, CypD-independent effect of C31 on mPTP opening  
486 is not ubiquinone-like.

487           Because it has been reported that inhibiting complex I with rotenone limits mPTP  
488 opening<sup>29</sup>, we investigated whether C31 has an effect on respiratory chain functions. C31 did  
489 not alter substrate-dependent respiration rates or ADP-induced O<sub>2</sub> consumption, suggesting no  
490 C31-induced alteration of mitochondrial respiration (Supplementary Figure 2). No drop in the  
491 electron transport chain activity (lower  $\Delta\Psi_m$  and slower calcium absorption) was detected in  
492 our experiments. Thus, the greater potency of C31 as compared to CsA in inhibiting mPTP  
493 opening is not related to an interaction with mitochondrial complex I or the respiratory chain.

494

495 ***SMCypI compound C31 inhibits mPTP opening in vivo in mice***

496

497           Anesthetized mice were infused with increasing doses of C31 for 3 min and sacrificed  
498 2 min later. Liver mitochondria were isolated and their calcium retention capacity was  
499 measured. Mitochondria isolated from C31-treated mouse livers exhibited higher calcium  
500 retention capacities than those from vehicle-treated mice, and this effect was dose-dependent.  
501 The effect of C31 was more potent than that of CsA (Figure 6A). This result, showing *in vivo*  
502 inhibition of mPTP opening by SMCypI compound C31, indicates that C31 reaches its  
503 mitochondrial target after infusion in living mice.

504

505 ***SMCypI compound C31 bears mito- and hepatoprotective properties during experimental***  
506 ***liver ischemia-reperfusion in mice***

507

508           Our final series of experiments aimed at demonstrating the protective effect of SMCypI  
509 compound C31 in an experimental murine model of hepatic ischemia-reperfusion injury. First,  
510 mice were subjected to 60 min of liver ischemia followed by 10 min of reperfusion. Ischemia-  
511 reperfusion reduced the calcium retention capacity of isolated mouse mitochondria by 59%  
512 (96.1±4.5 to 39.0±2.7 nmol/mg of protein; p <0.001). This reduction was associated with an

513 alteration of oxidative phosphorylation, as demonstrated by a 31% decrease of the rate of ADP-  
514 stimulated respiration ( $p=0.0016$  vs Sham) and a 52% decrease of the respiratory control ratio  
515 ( $p=0.0026$  vs Sham) (Figure 6B). Infusion of the most effective dose of C31 (150 mg/kg) 1 min  
516 before and during the first 8 min of reperfusion restored normal calcium retention capacity  
517 ( $84.9\pm 8.9$  nmol/mg of protein). The protective effect of C31 also translated into a restoration of  
518 oxidative phosphorylation parameters (Figure 6B).

519 Secondly, the hepatoprotective effect of C31 was assessed in mice subjected to 60 min  
520 of liver ischemia, followed by 60 min of reperfusion. Blood samples were collected for ALT  
521 and AST level measurement and livers were excised for liver histology assessment (Figure 7A).  
522 C31 treatment significantly reduced ischemia-reperfusion-induced ALT elevation at the end of  
523 reperfusion (mean ALT levels:  $2,297\pm 290$  versus  $4,805\pm 1,088$  in C31-treated and vehicle-  
524 treated mice, respectively;  $p=0.0375$ ) (Figure 7B). The effect of C31 on serum ALT levels was  
525 significantly greater than that of CsA, which was not significantly different from that of the  
526 vehicle (data not shown). C31 also substantially reduced AST elevation, but the difference did  
527 not reach significance (Supplementary Figure 3).

528 As shown in Figures 7C, 7D and 7E, C31 protected mouse livers from hepatic damages  
529 induced by ischemia-reperfusion. Indeed, 60 min after reperfusion, hepatic clarification areas  
530 that measure hepatocyte ballooning degeneration, a feature of acute liver injury (Figure 7D),  
531 covered a significantly smaller surface in C31-treated than in vehicle-treated mice ( $30.4\pm 4.3\%$   
532 versus  $50.7\pm 3.2\%$  of liver section surface, respectively;  $p=0.0012$ ). CsA also significantly  
533 reduced the surface of hepatic clarification in the model, to an extent similar to the effect of  
534 C31 (data not shown).

535 These findings indicate that SMCypI compound C31 exerts both mito- and  
536 hepatoprotective effects in mice exposed to ischemia-reperfusion.

537

## 538 Discussion

539

540 Hepatic ischemia-reperfusion injury is a major complication of liver surgery with  
541 limited therapeutic options. Ischemia-reperfusion injury results in great part from hepatic  
542 mitochondrial dysfunction related to abnormal mPTP opening. CypD is an important regulator  
543 of the mPTP complex that plays a key role in its opening in several pathological conditions,  
544 including hepatic ischemia-reperfusion<sup>11, 14</sup>. Indeed, CypD translocation to the inner  
545 mitochondrial membrane triggers mPTP opening and promotes cell death. Both effects can be  
546 prevented by pharmacological CypD inhibitors or CypD knock-out<sup>27, 30-32</sup>. Thus, CypD  
547 represents an attractive target for inhibition of mPTP opening and hepatocellular protection in  
548 the context of hepatic ischemia-reperfusion injury.

549 We designed a new family of SMCypIs made of two linked fragments binding the  
550 cyclophilin catalytic and gatekeeper pockets, respectively<sup>19</sup>. Our aim was to develop CypA  
551 inhibitors with antiviral activity against the hepatitis C virus. We showed that our SMCypIs  
552 bind CypA and potently inhibit both CypA PPIase activity and the replication of hepatitis C  
553 virus and related viruses in cell culture<sup>19, 33</sup>. Because the different cyclophilins are structurally  
554 very close (essentially differing by their cellular localizations and functions), we assessed  
555 whether the new SMCypIs inhibit CypD activity. As shown here, their inhibitory activity was  
556 potent and concentration-dependent. SMCypI compound C31 was the most potent CypD  
557 inhibitor in our experiments. Its cytotoxic concentration 50% was >100  $\mu$ M in Huh7 cells,  
558 suggesting a favorable therapeutic index<sup>19</sup>. We also showed that C31 binds both the catalytic  
559 and gatekeeper pockets of Cyp D.

560 The ability of our SMCypIs to inhibit mPTP opening and its mitochondrial  
561 consequences in a concentration-dependent manner correlated with their ability to block PPIase  
562 activity. Inhibition of mPTP opening was observed in different models and conditions,  
563 including energized and de-energized ones. This suggests that the SMCypIs act directly on  
564 CypD and mPTP opening, downstream of the site of action of the inducers used in the

565 experiments. Importantly, this effect was observed in both human and mouse primary  
566 hepatocytes, a result validating the human relevance of our findings.

567         Although the CypD affinity of the SMCypIs was lower than that of CsA, C31 achieved  
568 more potent mPTP opening inhibition than CsA at its maximum soluble concentration in the  
569 medium. Because non-immunosuppressive derivatives of CsA, e.g., PKF220-384 or NIM811,  
570 have been shown to be equipotent to CsA in inhibiting mPTP opening<sup>32</sup>, these compounds are  
571 also likely to have a weaker effect on mPTP opening than C31 (not tested). Importantly, our  
572 findings suggest that the additional effect of C31 on mPTP opening as compared to CsA is  
573 independent from CypD inhibition. Indeed, first, the concentrations of CsA and C31 that fully  
574 inhibited CypD PPIase activity retained the same amount of calcium in mitochondria; secondly,  
575 CsA did not alter the maximal calcium retention capacity induced by C31; thirdly, C31 had an  
576 effect on calcium accumulation in liver mitochondria isolated from *Ppif*<sup>-/-</sup> mice that do not  
577 express CypD.

578         The fact that CsA fully inhibited CypD PPIase activity in isolated mouse mitochondria  
579 (Supplementary Figure 3) suggests that the additional effect of C31 as compared to CsA is not  
580 related to its ability to inhibit PPIase activity. Because the structure and functioning of mPTP  
581 remain largely unknown, we could not identify the second target of C31 responsible for its  
582 greater potency as compared to CsA. We could however rule out an alteration of mitochondrial  
583 respiration<sup>29</sup> or a ubiquinone-like mechanism<sup>28</sup>. Many potential components or regulators of  
584 the mPTP, such as the recently identified SPG7<sup>34</sup>, could be involved, while many questions  
585 remain unanswered: is mPTP organized as a true physical channel? Is opening just a different  
586 state of the mitochondrial membrane with increased permeability? Which cellular components  
587 are actual constituents of the mPTP? Which ones only interact with it and/or regulate it? What  
588 are the mechanisms involved? Answering these questions was beyond the scope of our study,  
589 but we are confident that the new family of SMCypIs will be helpful in future mechanistic  
590 studies aimed at exploring these questions. Altogether, our result identify SMCypI C31 as a

591 particularly promising mPTP opening blocking agent, because its effect on mPTP opening  
592 related to CypD PPIase activity inhibition is enhanced by another complementary mechanism.

593 Key results in this study were obtained *in vivo* in murine models. We showed that C31  
594 rapidly reaches its target after systemic administration. This is particularly important in the  
595 context of ischemia-reperfusion, because mPTP was reported to open within the first minutes  
596 of reperfusion after ischemia<sup>8, 35</sup>. For this reason, proof-of-concept efficacy experiments were  
597 performed *in vivo* in a murine model of ischemia-reperfusion. The administration of C31 at  
598 reperfusion restored the mitochondrial function. In addition, ALT elevations and hepatic  
599 damage were significantly reduced in C31-treated mice, proving the hepatoprotective properties  
600 of the new SMCypI, as a result of mPTP opening inhibition.

601 In this study, liver damage was assessed by measuring “hepatocyte clarification”, i.e.  
602 hepatocyte ballooning degeneration, a feature of severe liver cell injury involving ATP  
603 depletion and a rise in intracellular calcium concentrations leading to a loss of cell volume  
604 control by plasma membranes and a disruption of the hepatocyte intermediate filament network.  
605 Hepatocyte ballooning degeneration has been observed in the early post-transplant period<sup>36-3839</sup>,  
606 and described as an important morphological characteristic of ischemia-reperfusion injury  
607 measuring the degree of liver damage<sup>40-42</sup>. As shown in Figure 7D in our model, hepatocyte  
608 ballooning degeneration was characterized by hepatocellular swelling, cytoplasm vacuolization  
609 and blebbing of the cell membrane. It was significantly improved by C31 administration in our  
610 murine model of ischemia-reperfusion injury. Because the half-life of C31 is short, requiring  
611 continuous infusion, it was not possible to determine how long the protective effects might last.  
612 Chemical, galenic and pharmacological optimization of the compounds is in progress and  
613 studies with more stable derivatives will be conducted to address this important question as part  
614 of future preclinical development.

615 In summary, we showed that our new family of small-molecule, non-peptidic  
616 cyclophilin inhibitors binds CypD and inhibits its PPIase activity, and that this effect is, at least

617 in part, responsible for their concentration-dependent inhibitory effect on calcium-induced  
618 swelling due to mPTP opening in both human and mouse hepatocytes. We also showed that the  
619 most potent SMCypI, compound C31, exerts an additional effect on mPTP opening,  
620 independent of its inhibitory effect on CypD, making it a promising pharmacological agent for  
621 hepatocellular protection in the context of diseases involving mitochondrial dysfunction related  
622 to abnormal mPTP opening. Finally, our study is the first to provide the *in vivo* proof-of-concept  
623 of mitochondrial and hepatocellular protection by SMCypI compound C31 in an experimental  
624 model of ischemia-reperfusion injury.

625 The new family of SMCypIs appears as a promising candidate for new drug  
626 development in the indication of hepatic protection in the context of warm ischemia-reperfusion  
627 after liver surgery. Whether similar protection can be obtained in the context of cold ischemia-  
628 reperfusion related to orthotopic liver transplantation remains to be assessed. Other applications  
629 in liver and non-hepatic diseases related to mPTP opening involving CypD deserve to be  
630 explored. They include chronic alcohol consumption, which enhances sensitivity to calcium-  
631 mediated mPTP opening and increases CypD expression<sup>43</sup>, drug-induced liver injury,  
632 myocardial ischemia-reperfusion, brain injury and neurodegenerative disorders.

633

634 **References**

635

- 636 1. Konishi T, Lentsch AB. Hepatic ischemia/reperfusion: mechanisms of tissue injury,  
637 repair, and regeneration. *Gene Expr* 2017;17:277-287.
- 638 2. Cannistra M, Ruggiero M, Zullo A, et al. Hepatic ischemia reperfusion injury: a  
639 systematic review of literature and the role of current drugs and biomarkers. *Int J Surg*  
640 2016;33 Suppl 1:S57-70.
- 641 3. Go KL, Lee S, Zendejas I, et al. Mitochondrial dysfunction and autophagy in hepatic  
642 ischemia/reperfusion injury. *Biomed Res Int* 2015;2015:183469.
- 643 4. Halestrap AP. What is the mitochondrial permeability transition pore? *J Mol Cell Cardiol*  
644 2009;46:821-31.
- 645 5. Friberg H, Wieloch T. Mitochondrial permeability transition in acute neurodegeneration.  
646 *Biochimie* 2002;84:241-50.
- 647 6. Kim JS, He L, Qian T, et al. Role of the mitochondrial permeability transition in apoptotic  
648 and necrotic death after ischemia/reperfusion injury to hepatocytes. *Curr Mol Med*  
649 2003;3:527-35.
- 650 7. Rauen U, de Groot H. New insights into the cellular and molecular mechanisms of cold  
651 storage injury. *J Investig Med* 2004;52:299-309.
- 652 8. Halestrap AP. A pore way to die: the role of mitochondria in reperfusion injury and  
653 cardioprotection. *Biochem Soc Trans* 2010;38:841-60.
- 654 9. Rao VK, Carlson EA, Yan SS. Mitochondrial permeability transition pore is a potential  
655 drug target for neurodegeneration. *Biochim Biophys Acta* 2014;1842:1267-72.
- 656 10. Jaeschke H, McGill MR, Ramachandran A. Oxidant stress, mitochondria, and cell death  
657 mechanisms in drug-induced liver injury: lessons learned from acetaminophen  
658 hepatotoxicity. *Drug Metab Rev* 2012;44:88-106.

- 659 11. Giorgio V, von Stockum S, Antoniel M, et al. Dimers of mitochondrial ATP synthase  
660 form the permeability transition pore. *Proc Natl Acad Sci USA* 2013;110:5887-92.
- 661 12. Wang P, Heitman J. The cyclophilins. *Genome Biol* 2005;6:226.
- 662 13. Davis TL, Walker JR, Campagna-Slater V, et al. Structural and biochemical  
663 characterization of the human cyclophilin family of peptidyl-prolyl isomerases. *PLoS*  
664 *Biol* 2010;8:e1000439.
- 665 14. Javadov S, Kuznetsov A. Mitochondrial permeability transition and cell death: the role  
666 of cyclophilin D. *Front Physiol* 2013;4:76.
- 667 15. Griffiths EJ, Halestrap AP. Protection by cyclosporin A of ischemia/reperfusion-induced  
668 damage in isolated rat hearts. *J Mol Cell Cardiol* 1993;25:1461-9.
- 669 16. Matsuda S, Koyasu S. Mechanisms of action of cyclosporine. *Immunopharmacology*  
670 2000;47:119-25.
- 671 17. Azzolin L, Antolini N, Calderan A, et al. Antamanide, a derivative of *Amanita phalloides*,  
672 is a novel inhibitor of the mitochondrial permeability transition pore. *PLoS One*  
673 2011;6:e16280.
- 674 18. Piot C, Croisille P, Staat P, et al. Effect of cyclosporine on reperfusion injury in acute  
675 myocardial infarction. *N Engl J Med* 2008;359:473-81.
- 676 19. Ahmed-Belkacem A, Colliandre L, Ahnou N, et al. Fragment-based discovery of a new  
677 family of non-peptidic small-molecule cyclophilin inhibitors with potent antiviral  
678 activities. *Nat Commun* 2016;7:12777.
- 679 20. Pons JL, Labesse G. @TOME-2: a new pipeline for comparative modeling of protein-  
680 ligand complexes. *Nucleic Acids Res* 2009;37:W485-91.
- 681 21. Miteva MA, Guyon F, Tuffery P. Frog2: efficient 3D conformation ensemble generator  
682 for small compounds. *Nucleic Acids Res* 2010;38:W622-7.

- 683 22. Fontaine E, Eriksson O, Ichas F, et al. Regulation of the permeability transition pore in  
684 skeletal muscle mitochondria. Modulation by electron flow through the respiratory chain  
685 complex I. *J Biol Chem* 1998;273:12662-8.
- 686 23. Seglen PO. Preparation of isolated rat liver cells. *Methods Cell Biol* 1976;13:29-83.
- 687 24. Petronilli V, Miotto G, Canton M, et al. Transient and long-lasting openings of the  
688 mitochondrial permeability transition pore can be monitored directly in intact cells by  
689 changes in mitochondrial calcein fluorescence. *Biophys J* 1999;76:725-34.
- 690 25. Petronilli V, Penzo D, Scorrano L, et al. The mitochondrial permeability transition,  
691 release of cytochrome C and cell death. Correlation with the duration of pore openings in  
692 situ. *J Biol Chem* 2001;276:12030-4.
- 693 26. Bankhead P, Loughrey MB, Fernandez JA, et al. QuPath: open source software for digital  
694 pathology image analysis. *Sci Rep* 2017;7:16878.
- 695 27. Baines CP, Kaiser RA, Purcell NH, et al. Loss of cyclophilin D reveals a critical role for  
696 mitochondrial permeability transition in cell death. *Nature* 2005;434:658-62.
- 697 28. Walter L, Miyoshi H, Lerverve X, et al. Regulation of the mitochondrial permeability  
698 transition pore by ubiquinone analogs. A progress report. *Free Radic Res* 2002;36:405-  
699 12.
- 700 29. Li B, Chauvin C, De Paulis D, et al. Inhibition of complex I regulates the mitochondrial  
701 permeability transition through a phosphate-sensitive inhibitory site masked by  
702 cyclophilin D. *Biochim Biophys Acta* 2012;1817:1628-34.
- 703 30. Nakagawa T, Shimizu S, Watanabe T, et al. Cyclophilin D-dependent mitochondrial  
704 permeability transition regulates some necrotic but not apoptotic cell death. *Nature*  
705 2005;434:652-8.
- 706 31. Hansson MJ, Mattiasson G, Mansson R, et al. The nonimmunosuppressive cyclosporin  
707 analogs NIM811 and UNIL025 display nanomolar potencies on permeability transition  
708 in brain-derived mitochondria. *J Bioenerg Biomembr* 2004;36:407-13.

- 709 32. Waldmeier PC, Feldtrauer JJ, Qian T, et al. Inhibition of the mitochondrial permeability  
710 transition by the nonimmunosuppressive cyclosporin derivative NIM811. *Mol Pharmacol*  
711 2002;62:22-9.
- 712 33. Nevers Q, Ruiz I, Ahnou N, et al. Characterization of the anti-hepatitis C virus activity of  
713 new nonpeptidic small-molecule cyclophilin inhibitors with the potential for broad anti-  
714 Flaviviridae activity. *Antimicrob Agents Chemother* 2018;62:e00126-18.
- 715 34. Shanmughapriya S, Rajan S, Hoffman NE, et al. SPG7 is an essential and conserved  
716 component of the mitochondrial permeability transition pore. *Mol Cell* 2015;60:47-62.
- 717 35. Glantzounis GK, Salacinski HJ, Yang W, et al. The contemporary role of antioxidant  
718 therapy in attenuating liver ischemia-reperfusion injury: a review. *Liver Transpl*  
719 2005;11:1031-47.
- 720 36. Lefkowitz JH. Scheuer's Liver biopsy interpretation. Edinburgh: Elsevier, 2016.
- 721 37. Neil DA, Hubscher SG. Delay in diagnosis: a factor in the poor outcome of late acute  
722 rejection of liver allografts. *Transplant Proc* 2001;33:1525-6.
- 723 38. Hubscher SG. Histological findings in liver allograft rejection: new insights into the  
724 pathogenesis of hepatocellular damage in liver allografts. *Histopathology* 1991;18:377-  
725 83.
- 726 39. Khettry U, Backer A, Ayata G, et al. Centrilobular histopathologic changes in liver  
727 transplant biopsies. *Hum Pathol* 2002;33:270-6.
- 728 40. Datta G, Fuller BJ, Davidson BR. Molecular mechanisms of liver ischemia reperfusion  
729 injury: insights from transgenic knockout models. *World J Gastroenterol* 2013;19:1683-  
730 98.
- 731 41. Saeed WK, Jun DW, Jang K, et al. Does necroptosis have a crucial role in hepatic  
732 ischemia-reperfusion injury? *PLoS One* 2017;12:e0184752.
- 733 42. Arab HA, Sasani F, Rafiee MH, et al. Histological and biochemical alterations in early-  
734 stage lobar ischemia-reperfusion in rat liver. *World J Gastroenterol* 2009;15:1951-7.

735 43. King AL, Swain TM, Dickinson DA, et al. Chronic ethanol consumption enhances  
736 sensitivity to Ca(2+)-mediated opening of the mitochondrial permeability transition pore  
737 and increases cyclophilin D in liver. *Am J Physiol Gastrointest Liver Physiol*  
738 2010;299:G954-66.

739

740

741 **Figure legends**

742

743 **Figure 1. (A)** Molecular modeling and docking of SMCypI compound C31 bound to the  
744 catalytic site (left) and gatekeeper pocket (right) of CypD. **(B)** Concentration-dependent  
745 inhibitory effect of SMCypI C31 on isolated mouse liver mitochondrial swelling. Swelling was  
746 induced by 50  $\mu\text{M}$  calcium in the absence of inhibitors, in the presence of 1  $\mu\text{M}$  CsA (positive  
747 control of inhibition) or in the presence of increasing (0.1 to 10  $\mu\text{M}$ ) concentrations of C31. No  
748 calcium was added in the negative control. The x axis indicates times of measurement; the y  
749 axis shows dynamic changes in absorbance at 540 nm ( $A_{540}$ ) reflecting changes in  
750 mitochondrial swelling. **(C)** Relationship between SMCypI inhibition of CypD PPIase activity  
751 in an enzyme assay and swelling of isolated mouse liver mitochondria.

752

753 **Figure 2.** Inhibitory effect of SMCypI C31 on mitochondrial swelling triggered by mPTP  
754 opening inducers in isolated mouse mitochondria incubated in the presence of  $\text{Ca}^{2+}$ . The x axis  
755 indicates times of measurement; the y axis shows dynamic changes in absorbance at 540 nm  
756 ( $A_{540}$ ) reflecting changes in mitochondrial swelling. **(A)** mPTP opening induced by 40  $\mu\text{M}$  *tert*-  
757 butyl hydroperoxide (*t*-BH) in energized mitochondria. **(B)** mPTP opening induced by 100  $\mu\text{M}$   
758 carboxyatractyloside (CAT) in energized mitochondria. **(C)** mPTP opening induced by 1  $\mu\text{M}$   
759 A23187 (A23) in non-energized mitochondria. **(D)** mPTP opening induced by 10  $\mu\text{M}$   
760 phenylarsine oxide (PAO) in non-energized mitochondria.

761

762 **Figure 3.** Inhibition of mPTP opening by CsA and SMCypI compound C31 in primary mouse  
763 and human hepatocytes. **(A)** Experimental procedure: hepatocytes were loaded with calcein and  
764  $\text{CoCl}_2$  and mPTP opening was induced by the addition of 1  $\mu\text{M}$  of the calcium ionophore  
765 A23187 (A23), in the absence (control) or in the presence of CsA or of increasing  
766 concentrations of C31. Images were collected at 1-min intervals. Fluorescence was normalized

767 to 100% of the maximal value. The results of 4 to 7 experiments were averaged. **(B)** Inhibition  
 768 of mPTP opening by CsA and SMCypI compound C31 in primary mouse hepatocytes. Left  
 769 curves: kinetics of calcein fluorescence over time; right bar graph: calcein fluorescence  
 770 measured at 30 min ( $\#p < 0.05$  vs A23 alone;  $*p < 0.05$  vs control;  $\dagger p < 0.05$  vs CsA) **(C)**  
 771 Inhibition of mPTP opening by CsA and SMCypI compound C31 in primary human  
 772 hepatocytes. Left curves: kinetics of calcein fluorescence over time; right bar graph: calcein  
 773 fluorescence measured at 30 min ( $\#p < 0.05$  vs A23 alone;  $*p < 0.05$  vs control (Ctrl);  $\dagger p < 0.05$   
 774 vs CsA).

775

776 **Figure 4.** Calcium retention capacity of isolated mouse liver mitochondria in the presence of  
 777 SMCypI compound C31 and of CsA. **(A)** Representative experiment showing mitochondrial  
 778 calcium retention capacity in the presence of 1  $\mu$ M CsA or increasing concentrations of C31.  
 779 Each fluorescence peak corresponds to the addition of 20  $\mu$ M calcium. **(B)** Average calcium  
 780 concentrations required for mPTP opening, expressed as a percentage of the control value  
 781 (100% represents  $109 \pm 15$   $\mu$ M, as indicated by the dashed line).  $*p < 0.05$  vs value observed with  
 782 0.1  $\mu$ M C31;  $\dagger p < 0.05$  vs 1  $\mu$ M CsA. CsA: cyclosporine A; AU: arbitrary unit; CRC: calcium  
 783 retention capacity; Ctrl: control.

784

785 **Figure 5.** Investigation of the mechanisms underlying the more potent effect of SMCypI  
 786 compound C31 on mitochondrial calcium retention capacity, as compared to CsA. **(A)**  
 787 Mean  $\pm$  SEM calcium retention capacity of isolated liver mitochondria from *Ppif*<sup>-/-</sup> (CypD  
 788 knocked-out) and wild-type mice. CRC: calcium retention capacity; WT: wild-type;  $\#p < 0.05$   
 789 vs wild-type control;  $*p < 0.05$  vs *Ppif*<sup>-/-</sup> and wild-type controls, respectively;  $\dagger p < 0.05$  vs CsA.  
 790 **(B)** Representative experiment showing the calcium concentrations required for mPTP opening  
 791 in liver mitochondria isolated from *Ppif*<sup>-/-</sup> mice in the absence of compounds (control) or in the  
 792 presence of 1  $\mu$ M CsA or 100  $\mu$ M C31. Each fluorescence peak corresponds to the addition of

793 20  $\mu$ M calcium. AU: arbitrary units. (C) Concentration-dependent C31 inhibition of  
794 mitochondrial swelling induced by 500  $\mu$ M calcium in liver mitochondria isolated from *Ppif*<sup>-/-</sup>  
795 mice. A<sub>540</sub>: absorbance at 540 nm. (D) Effect of 100  $\mu$ M C31 and C34 (a C31 derivative lacking  
796 the aromaticity of its phenyl moiety) on mitochondrial calcium retention capacity in isolated liver  
797 mitochondria from *Ppif*<sup>-/-</sup> mice. Each fluorescence peak corresponds to the addition of 20  $\mu$ M  
798 calcium. AU: arbitrary units. (E) Left: representative experiments showing the effect of 50  $\mu$ M  
799 C31 and 50  $\mu$ M ubiquinone 0 on mPTP opening in liver mitochondria isolated from wild-type  
800 (top) and *Ppif*<sup>-/-</sup> (bottom) mice. Each fluorescence peak corresponds to the addition of 20  $\mu$ M  
801 calcium. Right: Mean $\pm$ SEM calcium retention capacity (CRC) in the corresponding  
802 experiments. WT: wild-type; Ubo: ubiquinone 0; AU: arbitrary units; \**p* <0.05 vs control (Ctrl).  
803

804 **Figure 6.** *In vivo* effect of C31 on mPTP opening and mitochondrial alterations related to liver  
805 ischemia-reperfusion. (A) Anesthetized mice were infused with vehicle (VEH), CsA or  
806 different doses of C31 for 3 min and were sacrificed 2 min later. Liver mitochondria were  
807 isolated and the calcium retention capacities (CRC) of these mitochondria are shown. \**p* <0.05  
808 vs VEH; #*p* <0.05 vs CsA. (B) The mice were subjected to 60 min of a 70% partial liver  
809 ischemia, followed by 10 min of reperfusion, and received either 150 mg/kg C31 or vehicle  
810 (VEH). At the end of the reperfusion period, mouse livers were excised and mitochondria were  
811 isolated to assess the CRC (left) and mitochondrial respiration parameters (right), including the  
812 ADP-stimulated respiration rate (state 3), the substrate-dependent respiration rate (state 4) and  
813 the respiratory control ratio (RCR: state 3/state 4). \**p* <0.05 vs sham.

814

815 **Figure 7.** *In vivo* hepatoprotective effect of C31 in the context of liver ischemia-reperfusion.  
816 (A) The mice were subjected to 60 min of a 70% partial liver ischemia, followed by 60 min of  
817 reperfusion; they received either 150 mg/kg C31 or vehicle (VEH). At the end of the reperfusion  
818 period, blood samples and mouse livers were collected for assessment of liver damage. (B)

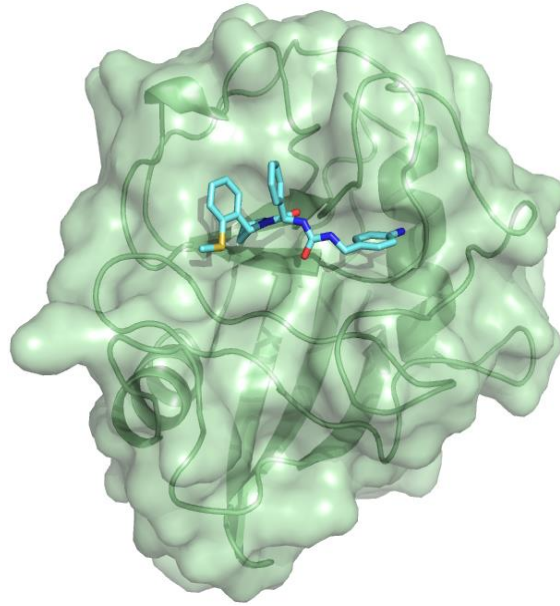
819 Mean±SEM ALT levels 60 min after reperfusion in VEH- and C31-treated animals; \*p <0.05.  
820 **(C)** Proportion of liver section surface occupied by hepatocyte clarification in VEH- and C31-  
821 treated animals; \*p <0.05. **(D)** Morphological alterations of hepatocyte clarification or hepatic  
822 ballooning degeneration : A shows hepatocyte swelling and cytoplasmic clarification; B shows  
823 cytoplasmic vacuolisation; C shows diffuse cell borders, an indirect feature of blebbing cell  
824 membrane. **(E)** Representative hematoxylin-eosin-stained liver sections from VEH- and C31-  
825 treated groups.

826

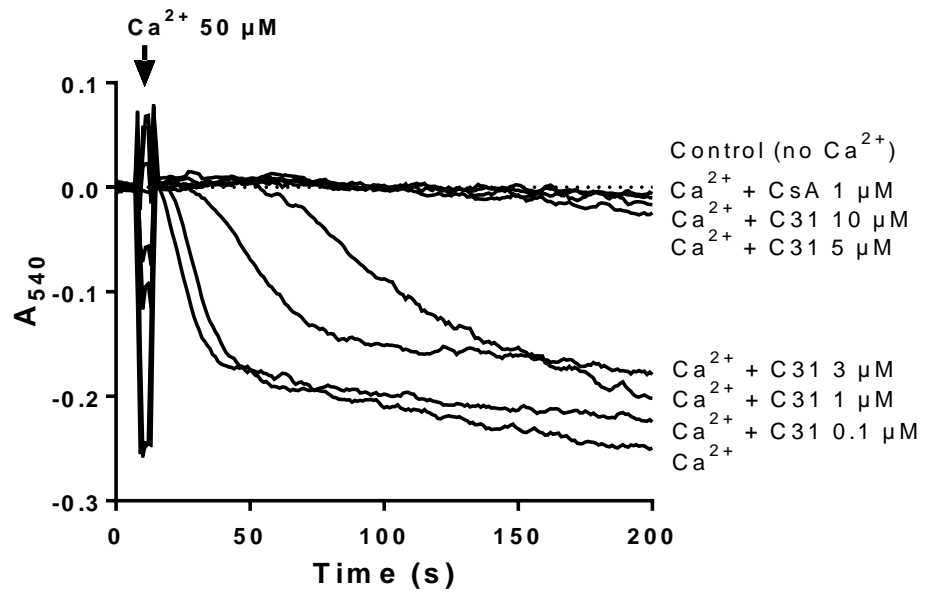
827

Fig. 1

**A**



**B**



**C**

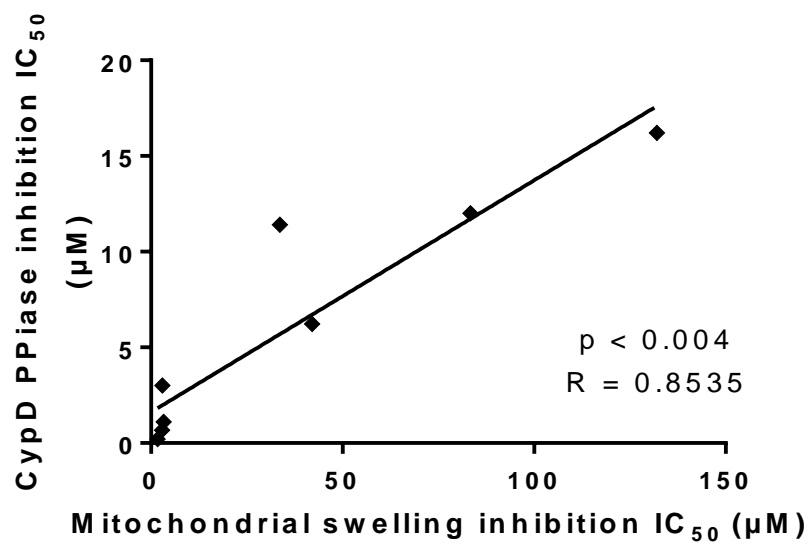
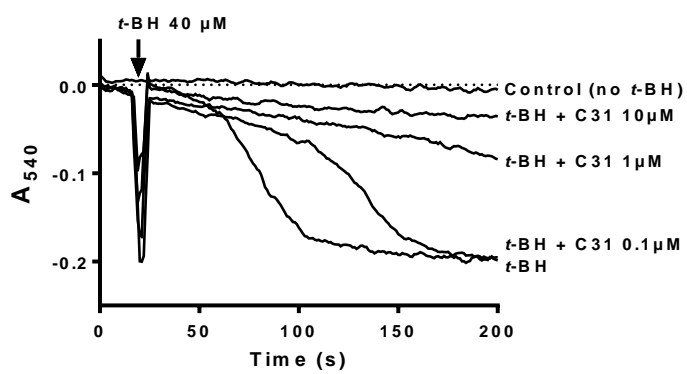
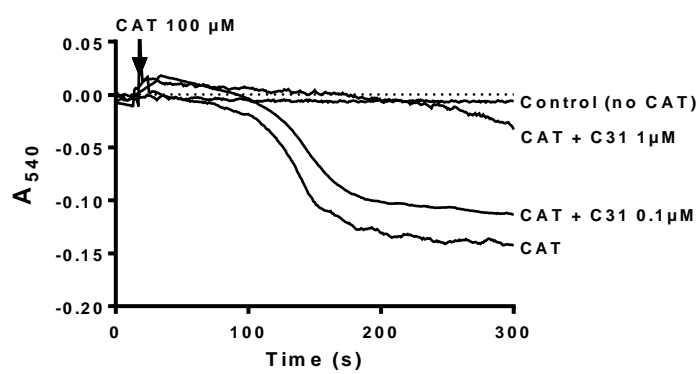


Fig. 2

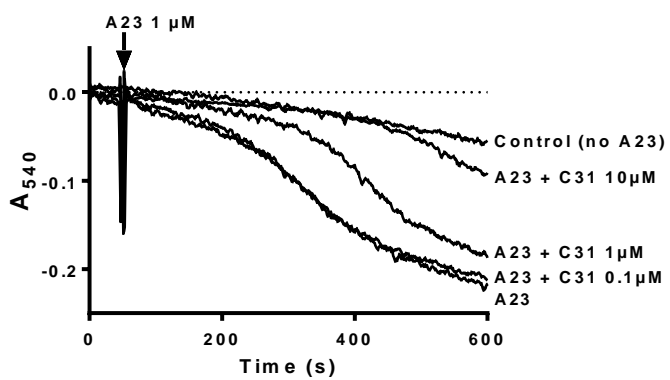
**A**



**B**



**C**



**D**

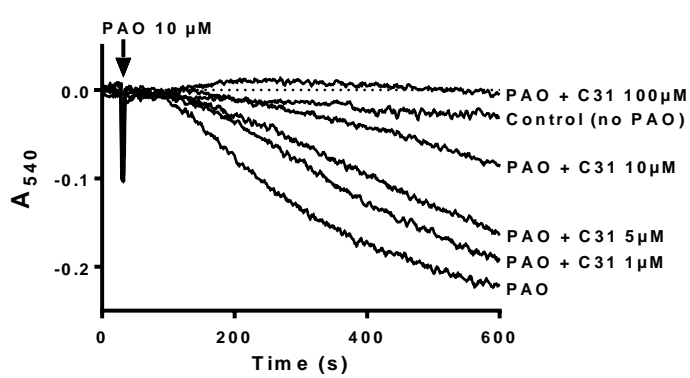
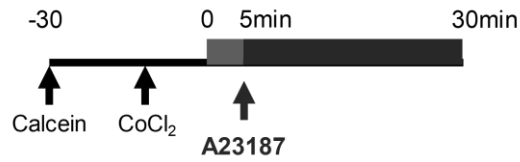


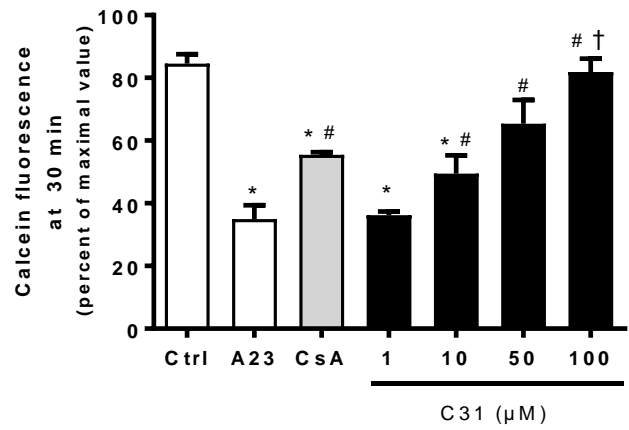
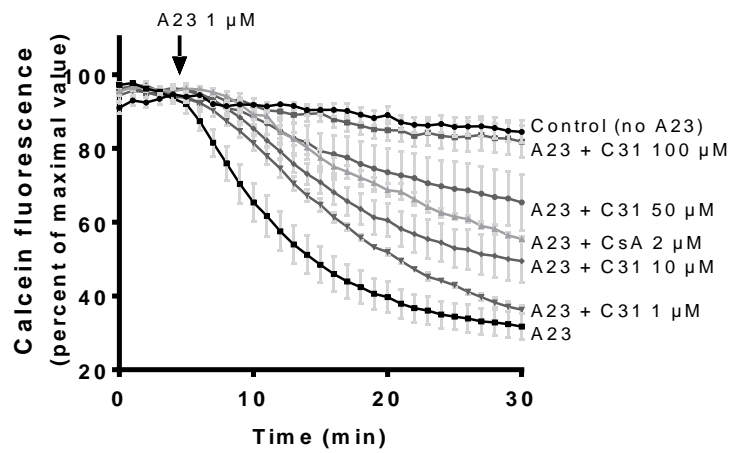
Fig. 3

**A**



**B**

### Primary mouse hepatocytes



**C**

### Primary human hepatocytes

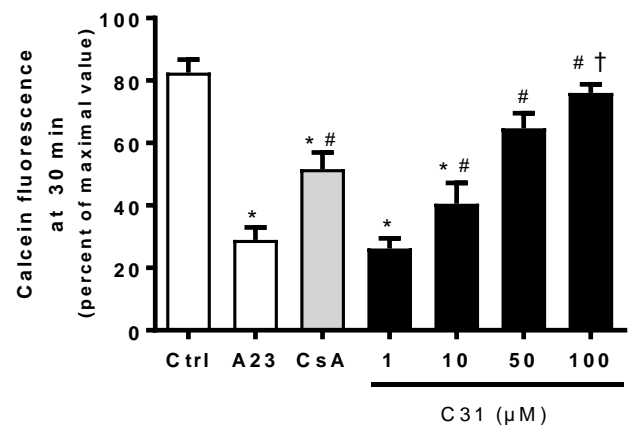
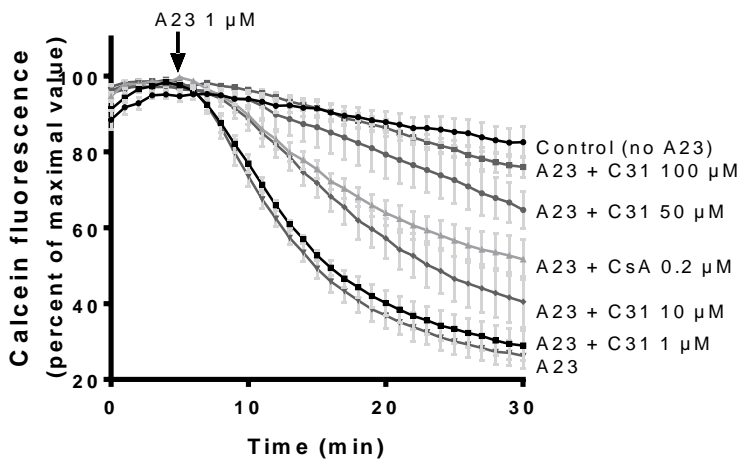


Fig. 4

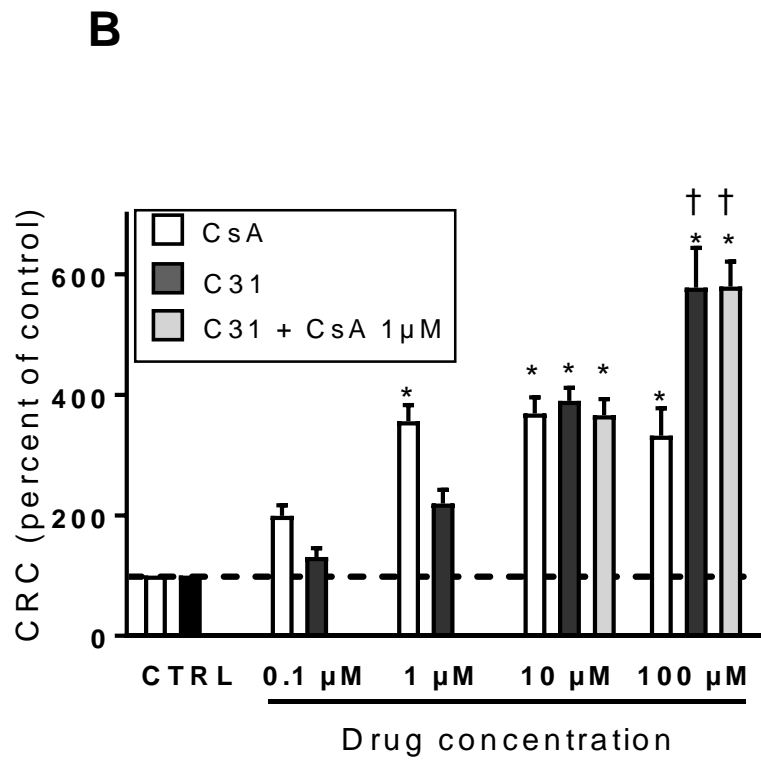
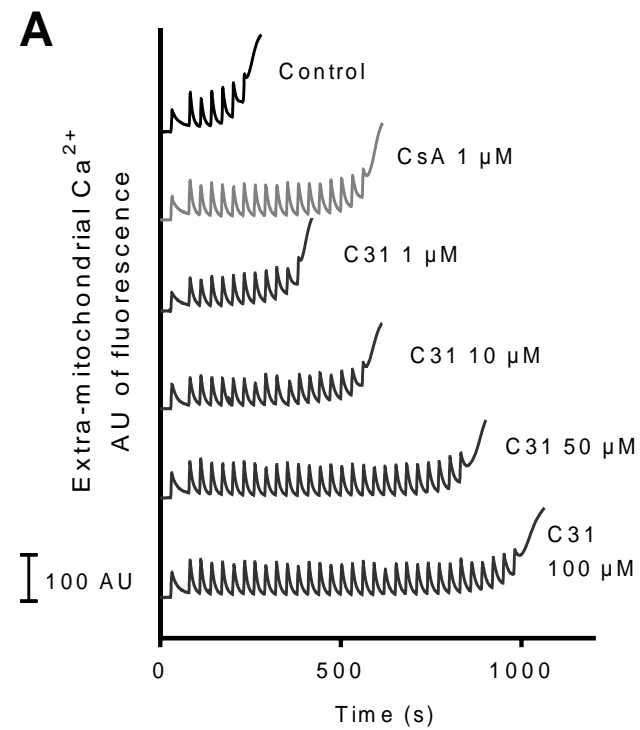
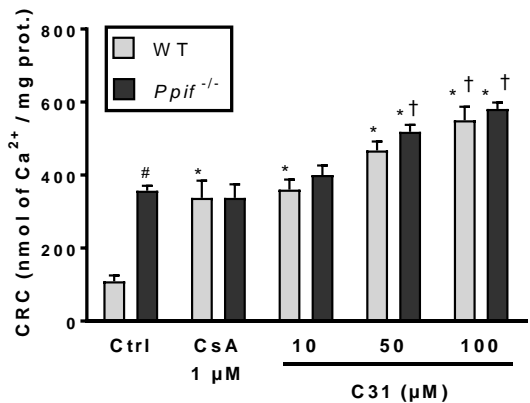
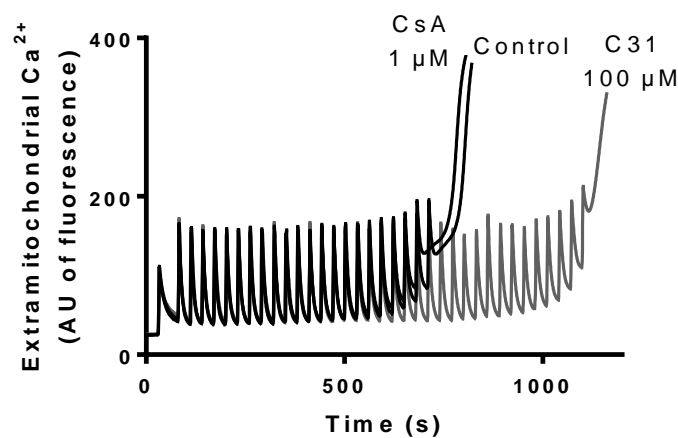


Fig. 5

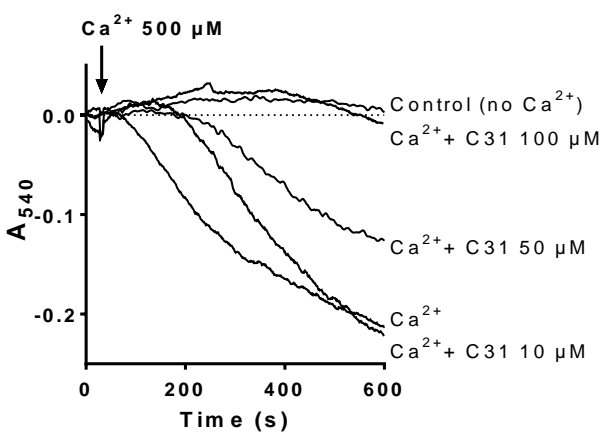
**A**



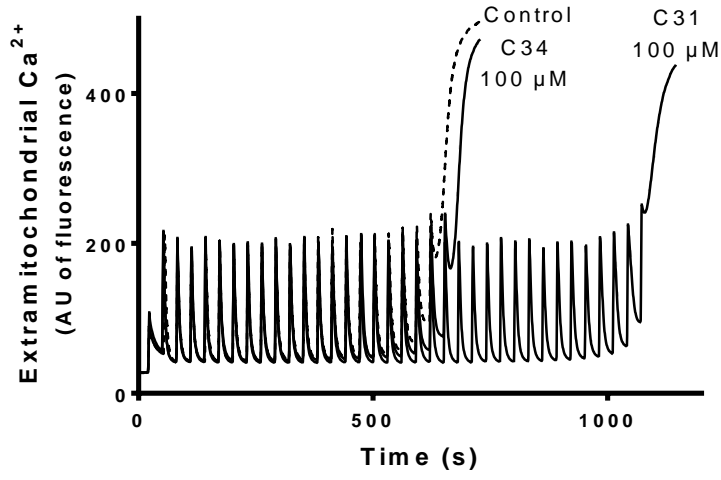
**B**



**C**



**D**



**E**

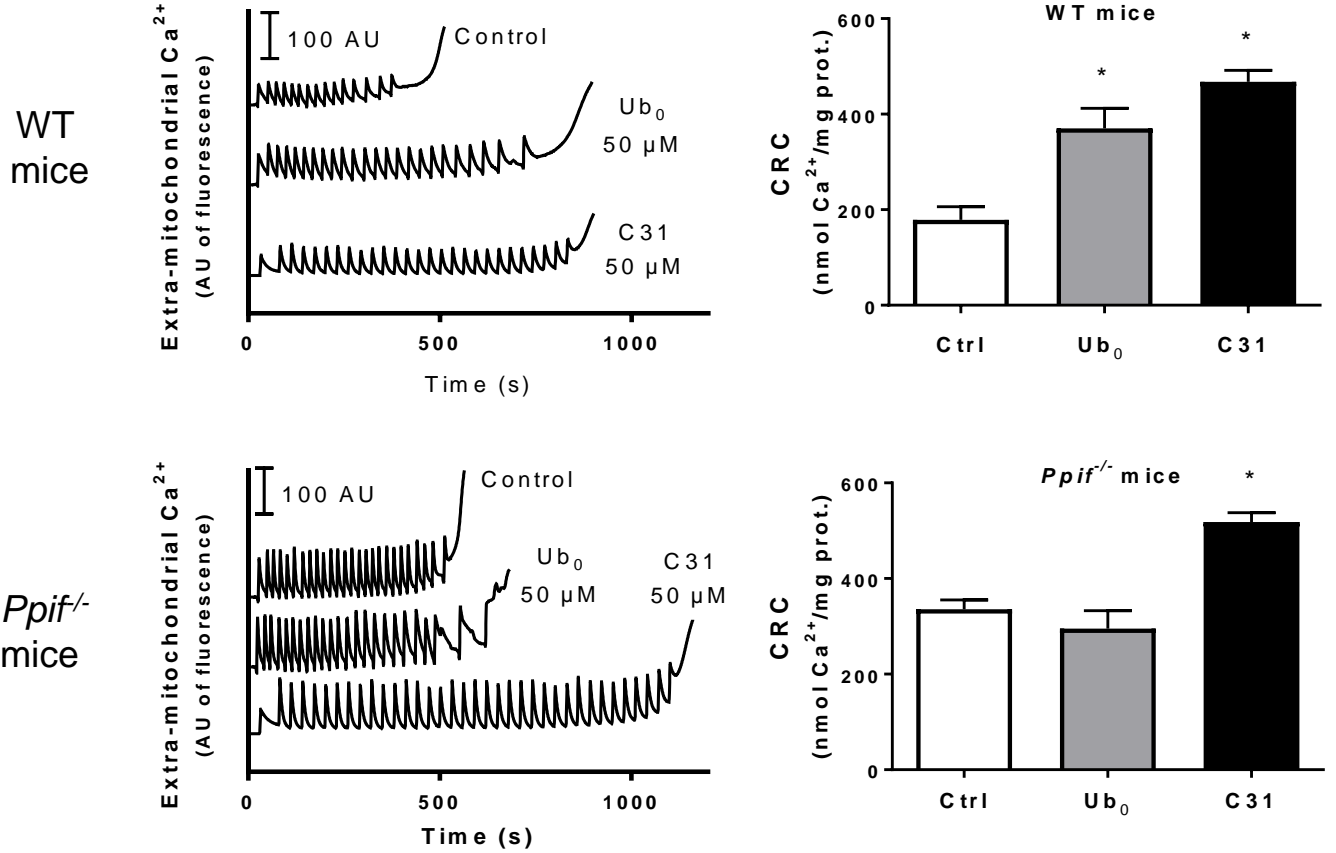


Fig. 6

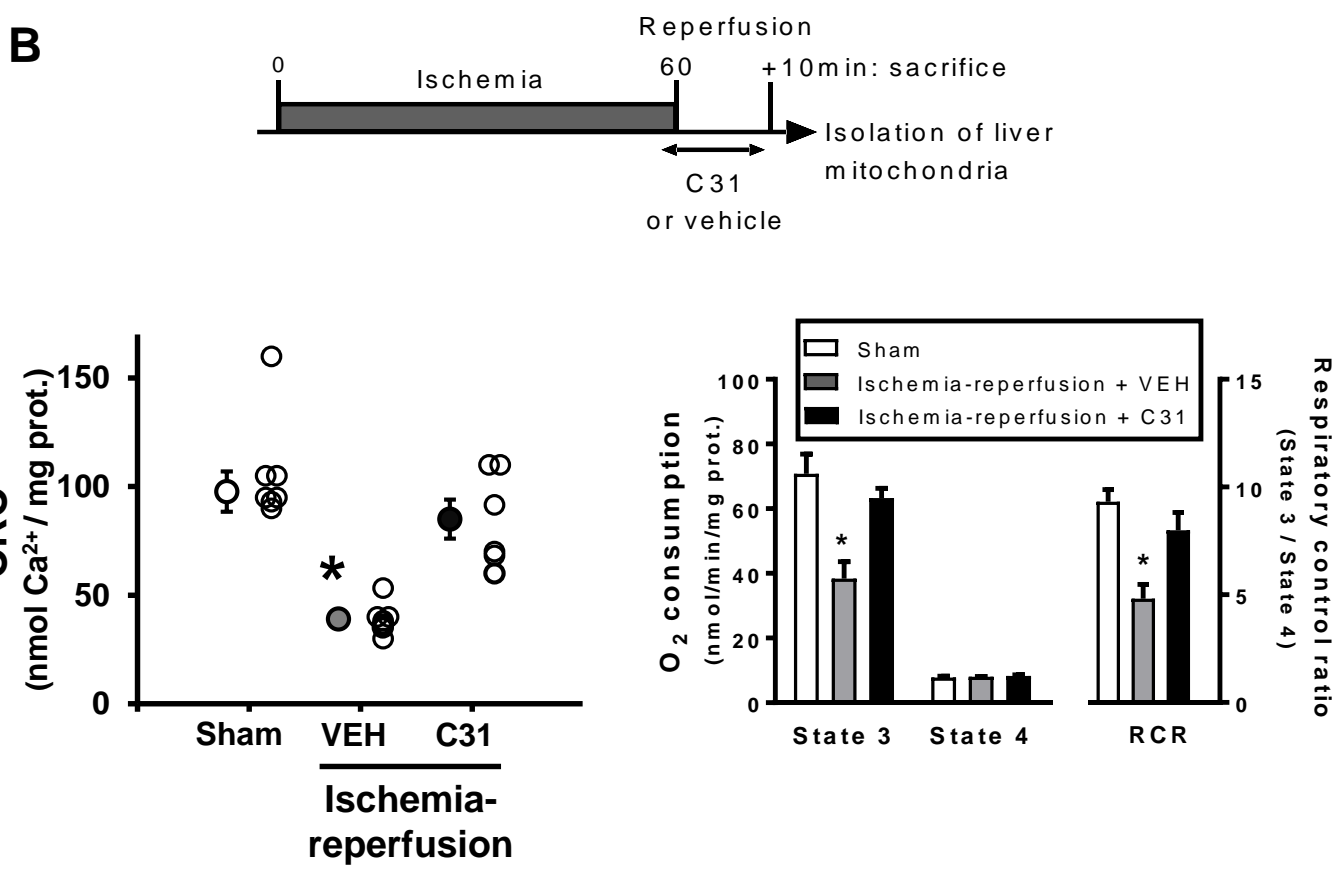
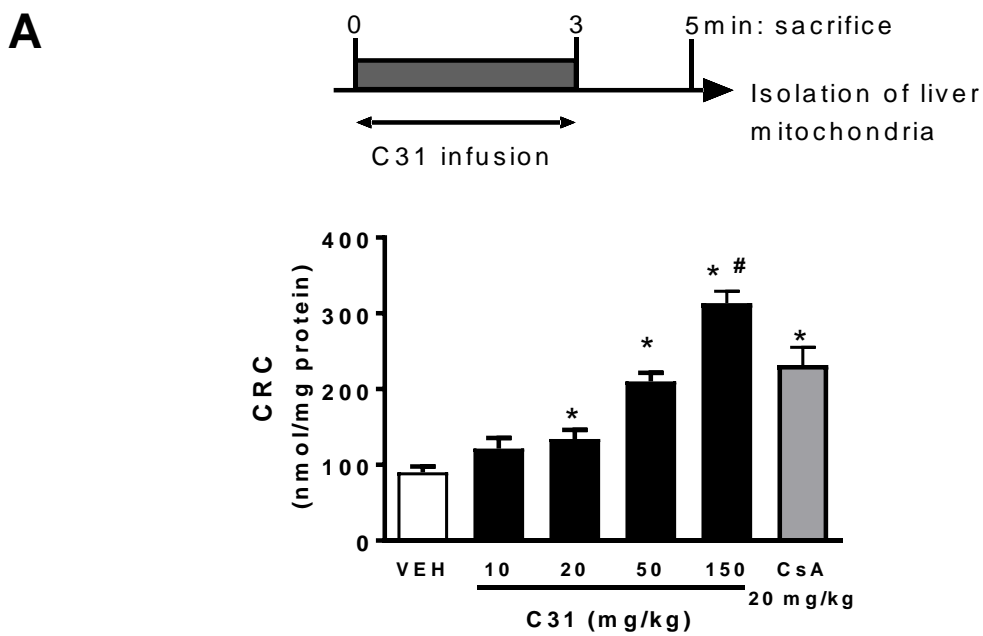


Fig. 7

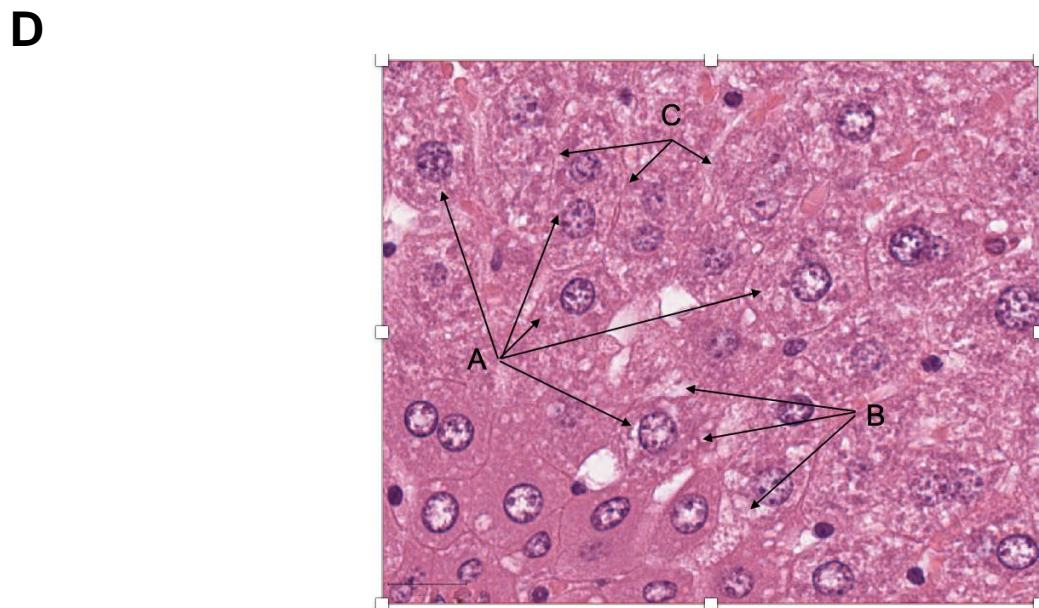
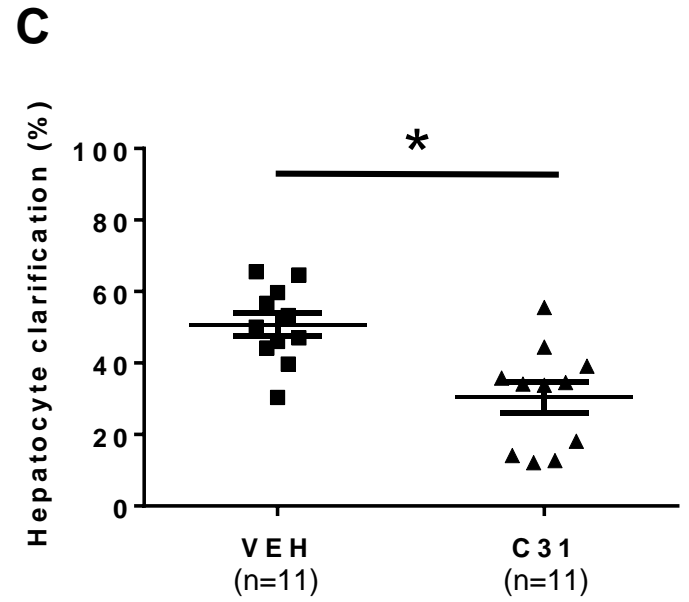
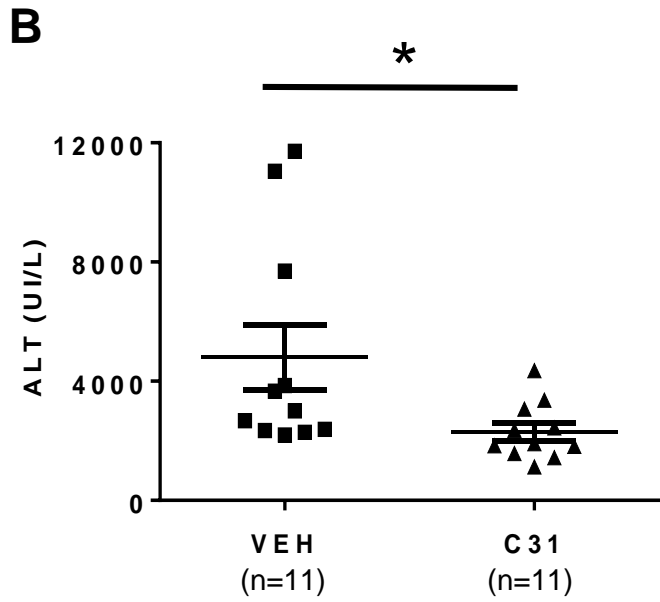
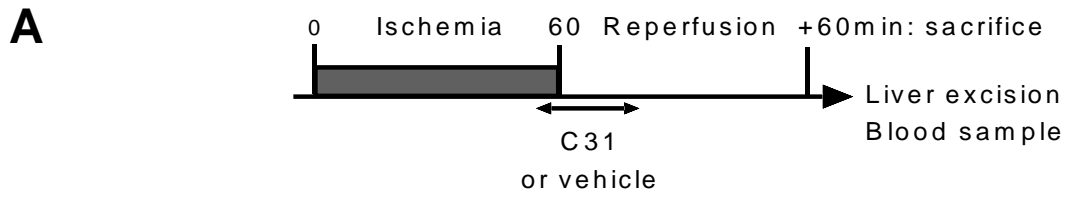


Fig. 7 (continued)

**E**

